Structural Selection and Amorphization of Small Ni−Ti Bimetallic Clusters

H. B. Liu,[†] G. Canizal,[‡] P. S. Schabes-Retchkiman,[§] and J. A. Ascencio*,[†]

*Programa de Investigación en Ductos, Corrosion y Materiales, Instituto Mexicano del Petroleo,
Eje Central Lázaro Cárdenas 152, Col. San Bartolo Atepehuacan, C.P. 07730, Mexico D.F., Mexico,
CECyD (Unidad Allende), Instituto Politécnico Nacional, Allende No. 38, Centro, México D.F. C.P. 06010,
México, and Instituto de Física, Universidad Nacional Autonoma de Mexico, Apartado Postal 20-364, Mexico,
Distrito Federal, C.P. 01000, México*

Classical molecular dynamics simulation is used for structural thermodynamic analysis of Ni−Ti bimetallic clusters. Experimental observation for the nanoclusters synthesized by the bioreduction method is used to consolidate the conclusion. The results demonstrate that Ni−Ti nanoclusters as small as 2−3 nm are not energetically favorable for common ordered geometrical arrangements such as cuboctahedron, decahedron, and icosahedron, though they can be synthesized experimentally. For the elemental distribution, Ni and Ti tend to aggregate separately. In the cases under study, eutectic-like and Ni-core/Ti-shell structures can keep their basic shape and elemental distribution during long periods of relaxation at room temperature. For other cases such as solid solution and Ti-core/Ni-shell, the structures amorphized and the elements tend to distribute uniformly even though they are at temperatures as low as room temperature. Experimental evidence was obtained by the analysis of biosynthesized nanoparticles using transmission electron microscopy techniques. This allowed determination of the partial amorphized structures of small bimetallic particles with cubic and multiple twined-like structures.

1. Introduction

NiTi shape memory alloys[1] are very interesting because of their remarkable shape memory effect, pseudoelasticity, and other excellent properties. Besides bulk NiTi materials, NiTi particles are also of great interest to researchers. Jardine et al.[2] produced particles by plasma spray in a vacuum. Cui et al.[3] produced NiTi particles by hydrogenation and ball milling. Liang et al.,[4,5] Porter et al.,[6] and Gu et al.[7] produced amorphous NiTi materials by mechanical alloying. Zhao et al. produced NiTi particles in nanoscale by chemical reaction in molten salts.[8] Schabes et al. produced NiTi nanoparticle as small as a few nanometers by a bioreduction method.[9] On the other hand, it has been reported that Ni−Ti intermetallic compounds could undergo a crystalline-to-amorphous (C−A) transformation upon irradiation,[10] and molecular dynamics (MD) studies have shown that the introduction of either chemical disordering or point defects into the crystalline lattices of the compounds could result in a C−A transition.[11,12] The use of high-resolution transmission electron microscopy has allowed an important capacity to determine the structure of small aggregates, and together with simulation methods it allows associating the internal structure of nanoparticles to local configuration[13,14] and dynamic reordering arraying.[15,16] Interestingly, in the Ni−Ti system, sharply different irradiation effects have been observed for three intermetallic compounds, i.e., the NiTi and NiTi$_2$ phases underwent amorphization, while the Ni-rich Ni$_3$Ti phase transformed into a solid solution upon ion irradiation.[17−20] In this

work, classical molecular dynamics simulations are used to clarify thermodynamically the structural selection and elemental distribution for Ni−Ti nanoclusters as small as 2−3 nm, meanwhile the amorphization was also studied.

2. Research Methods

2.1. Simulation Methods. For the Ni−Ti system, Farkas et al.[21] developed an embedded atom method. However, the application of the potential on MD simulation is unable to reproduce the experimentally observed solid-state amorphization in the Ni−Ti multilayers and the potential cannot predict that the martensitic phase is more stable than the B2 phase at low-temperature either. Lai et al.[22] developed an improved interaction potential based on the second-moment approximation of the tight-binding theory.[23] The cohesive energies and the lattice constants of some other Ni−Ti metastable and equilibrium crystalline phases are reproduced by the constructed potential agreed with those from first principle calculations[24] or experimental studies.[25,26] Obviously, for the NiTi phase at 0 K, the potential predicts that the martensitic phase possesses the largest cohesive energy, which is 0.018 and 0.118 eV/atom greater than those of B2 and L1$_0$, respectively. The potential is also able to reproduce the cohesive energy and lattice constants at 0 K for the Ni$_3$Ti phase, even though these experimental values were not used in the fitting procedure. Besides, the cohesive energy of the Ni$_3$Ti phase is derived by the potential to be 0.01 eV larger than that of L1$_2$ Ni$_3$Ti, revealing an energetic sequence of these two phases that is compatible with reality. Lai et al.[22] further verified the potential by some other thermodynamic properties based on MD simulations, e.g., enthalpy and volume, of the B2 NiTi phase. Consequently, the computed melting point is in excellent agreement with the experimental one. On the basis of the above consideration, we believe that the potential of Lai

* To whom all correspondence may be sent: E-mail: ascencio@imp.mx. Phone: +52 55 91758461. Fax: +52 55 91756429. http://www.paginasprodigy.com/jascenciogtz/.
† Programa de Investigación en Ductos, Corrosion y Materiales, Instituto Mexicano del Petroleo.
‡ CECyD (Unidad Allende), Instituto Politécnico Nacional.
§ Instituto de Física, Universidad Nacional Autonoma de Mexico.

12334 *J. Phys. Chem. B, Vol. 110, No. 25, 2006*

Liu et al.

TABLE 1: The Formation Energy of Ni−Ti Bimetal Cuboctahedral Clusters with 309 Atoms at 298 K
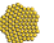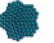
Morphology	Type of structure	component	Total cohesive energy, eV	Total formation energy of bimetal, eV
	Pure Ni	309 Ni 0 Ti	-4.155552	0
	Pure Ti	0 Ni 309 Ti	-4.597108	0
	Eutectic-like	147 Ni 162 Ti	-4.346683	12.47259
	Eutectic-like	162 Ni 147 Ti	-4.339175	8.16923
	Solid solution	147 Ni 162 Ti	-4.232626	47.71621
	Solid solution	162 Ni 147 Ti	-4.215658	46.33598
	Ni-Core/Ti-shell	147 Ni 162 Ti	-4.301456	26.44774
	Ti-Core/Ni-Shell	147 Ni 162 Ti	-4.219576	45.12532
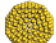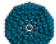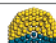
TABLE 2: The Formation Energy of Ni−Ti Bimetal Decahedral Clusters with 262 Atoms at 298 K
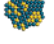
Morphology	Type of structure	component	Total cohesive energy, eV	Total formation energy of bimetal, eV
	Pure Ni	262 Ni 0 Ti	-4.127561	0
	Pure Ti	0 Ni 262 Ti	-4.544238	0
	Eutectic-like	99 Ni 163 Ti	-4.351619	9.21515
	Eutectic-like	163 Ni 99 Ti	-4.252182	8.60032
	Solid solution	99 Ni 163 Ti	-4.271421	30.22703
	Solid solution	163 Ni 99 Ti	-4.115722	44.35284
	Ni-Core/Ti-shell	99 Ni 163 Ti	-4.315607	18.6503
	Ti-Core/Ni-Shell	163 Ni 99 Ti	-4.165415	31.33327

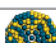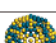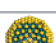**TABLE 3: The Formation Energy of Ni−Ti Bimetal Icosahedral Clusters with 309 Atoms at 298 K**

Morphology	Type of structure	component	Total cohesive energy, eV	Total formation energy of bimetal, eV
	Pure Ni	309 Ni 0 Ti	-4.182736	0
	Pure Ti	0 Ni 309 Ti	-4.597098	0
	Eutectic-like	147 Ni 162 Ti	-4.360593	12.16883
	Eutectic-like	162 Ni 147 Ti	-4.322470	17.73341
	Solid solution	147 Ni 162 Ti	-4.231561	52.03972
	Solid solution	162 Ni 147 Ti	-4.193548	57.57031
	Ni-Core/Ti-shell	147 Ni 162 Ti	-4.311585	27.3123
	Ti-Core/Ni-Shell	147 Ni 162 Ti	-4.240484	43.06708

using an ultrasonic bath and centrifuged. The mixture is held at room temperature for 2 h and centrifuged for 30 min, then the reaction mixture is separated and the obtained colloidal solution is allowed to rest for 48 h.

Electron microscopy characterization included transmission electron microscopy (TEM), high-resolution transmission electron microscopy (HRTEM) characterization, and high angle annular dark field imaging (HADDF) in scanning transmission electron microscopy (STEM) mode and energy filtering. To prepare a sample for TEM analysis, a couple of drops were deposited in a copper grid covered with amorphous carbon. Electron microscopy was performed in a JEOL JEM-2010F FasTem microscope at IFUNAM. HRTEM images were obtained at the optimal defocus condition (Scherzer). Fast Fourier transform was obtained from the images to identify the crystalline structure of the particles and structure.

3. Results and Discussion

To study the profile of the structure of Ni−Ti bimetallic nanoclusters as small as 2−3 nm, three common geometrical configurations are built. They are a 309-atom cuboctahedron, a 262-atom decahedron, and a 309-atom icosahedron. Three possible types of elemental distributions are applied, eutectic-like, solid solution, and core/shell. The specified components are $Ni_{147}Ti_{162}$ and $Ti_{147}Ni_{162}$ for 309-atom cubocthedra and icosahedra and $Ni_{99}Ti_{163}$ and $Ti_{99}Ni_{163}$ for 262-atom decahedra. The specified compositions are selected according to the corresponding core/shell structure with a single-layer atom shell for two possible types: Ni-core/Ti-shell or Ti-core/Ni-shell. Besides, the nanoclusters with specified compositions are not dilute for either Ni or Ti, which behave more like bimetallic properties of nanoclusters. Each structure is shown in Tables 1, 2, and 3, respectively. For each model cluster, 3.2×10^7 time steps were run, each time step is 2×10^{-15} s. The long relaxation time can ensure that the initial configurations reach equilibrium even if the temperature of the system is as low as room temperature.

3.1. Thermodynamic Analysis. The built clusters were relaxed fully and the total energies per atom were calculated. All the results are for room temperature. On the basis of the total energy for alloying cluster and pure clusters of Ni and Ti,

et al. can be considered a realistic one in a large range of compositions. Therefore, it provides us with strong support for the reliability of this work. MD simulations are performed using XMD developed by Riffkin.[27]

2.2. Experimental Methods. Synthesis of small bimetallic particles of Ti^0/Ni^0 was improved from reactions that reduced Ti^{4+} and Ni^{3+} into clusters of Ti^0/Ni^0. These particles are based on biosynthesis. A suspension of powdered milled alfalfa (which was washed previously, dried, milled, again washed with HCl solution, and finally dried) in deionized water is prepared at a concentration of 5 mg/mL, using an ultrasonic bath to homogenize the suspension. The pH is controlled by means of a buffer solution. After the mixture is placed in an ultrasonic bath, it is then centrifuged. A solution of metallic ions of titanium and nickel, previously prepared, with a concentration of 2.5×10^{-4} M is added, where the states of oxidation of the titanium and nickel are IV and III, respectively. The metallic solutions are prepared from a corresponding complex salt or nitrate salt, in distilled and deionized water, and mixed. Both solutions, the suspension and the metallic solution, are mixed homogeneously

Ni−Ti Bimetallic Clusters

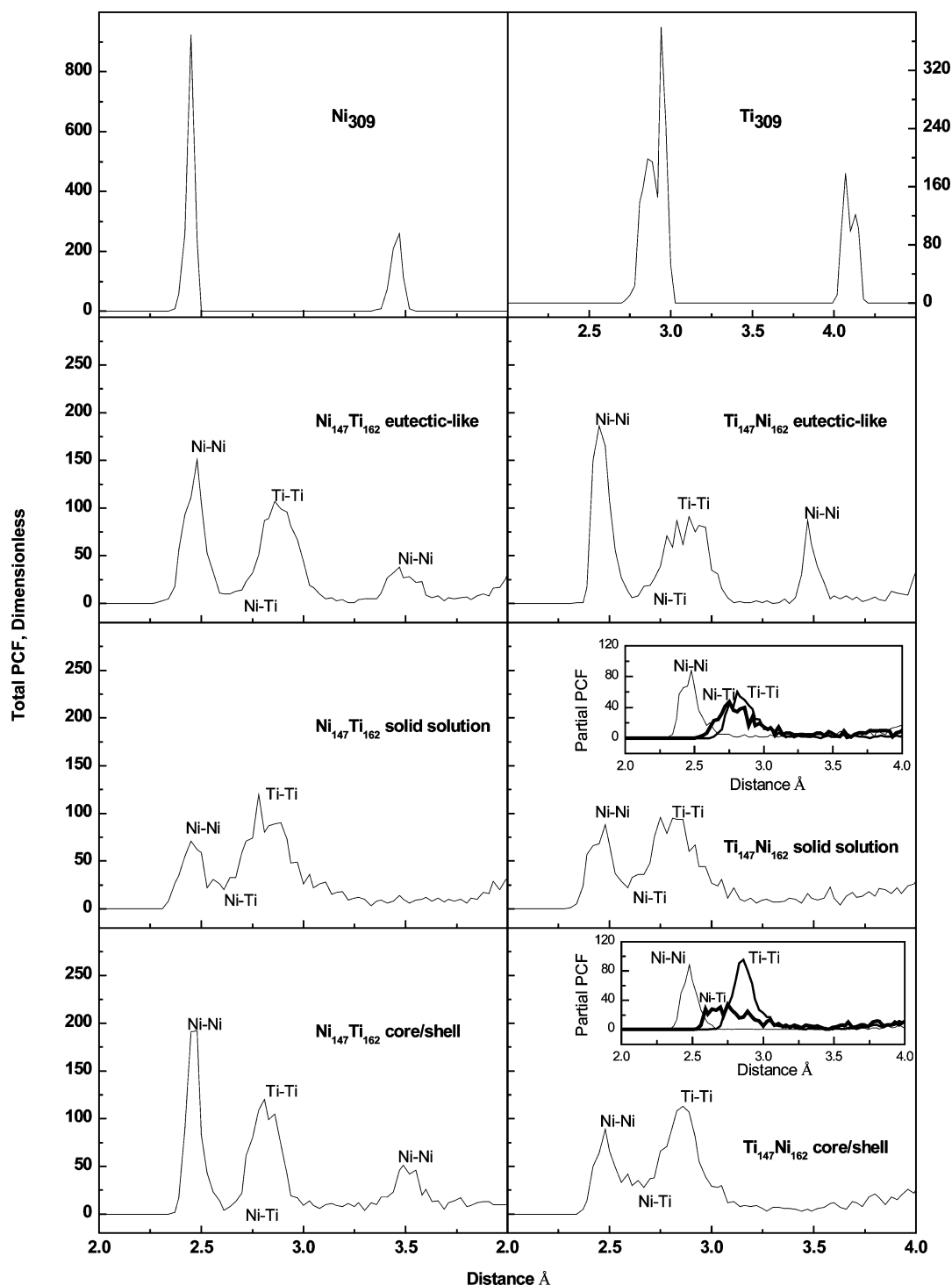*J. Phys. Chem. B, Vol. 110, No. 25, 2006* **12335**

Figure 1. Total and partial pair correlation function (PCF) for 309-atom cuboctahedron at 298 K.

the total formation energy of bimetallic cluster can be derived. Tables 1, 2, and 3 are the results for cubocthedra, decahedra, and icosahedra, respectively. In general, for whatever structure, cuboctahedra, decahedra, and icosahedra, the total formation energies of bimetallic nanoclusters are positive, which indicates that all the alloying clusters under study are not energetically favorable. That is to say, Ni−Ti clusters of 2−3 nm are not stable thermodynamically. Even if they are not stable, it is still possible that they can be synthesized and can coexist in some kinetic conditions. Therefore analysis of the stability for different types of structures is still interesting. It is not hard to find that for cuboctahedra, decahedra, and icosahedra, the most stable clusters are eutectic-like, the next is Ni-core/Ti-shell, and the

most unstable are solid solution and Ti-core/Ni-shell. It is noteworthy that the Ni−Ti nanoclusters behave very differently from their bulk alloy. As well known, Ni−Ti is a strong chemical order system and can form a few kinds of compounds depending on the compositions. For the preference for atom geometric arrangement in the case of similar elemental distribution, the decahedra have less positive values in bimetallic formation energy though its size is smaller. It demonstrates that decahedron is the most preferable geometrical configuration in comparison with cuboctahedra and icosahedra. The cuboctahedra and icosahedra have the same number of atoms; their stability can be compared directly. As a result, the cuboctahedra are more stable than icosahedra in the case of similar elemental distribu-
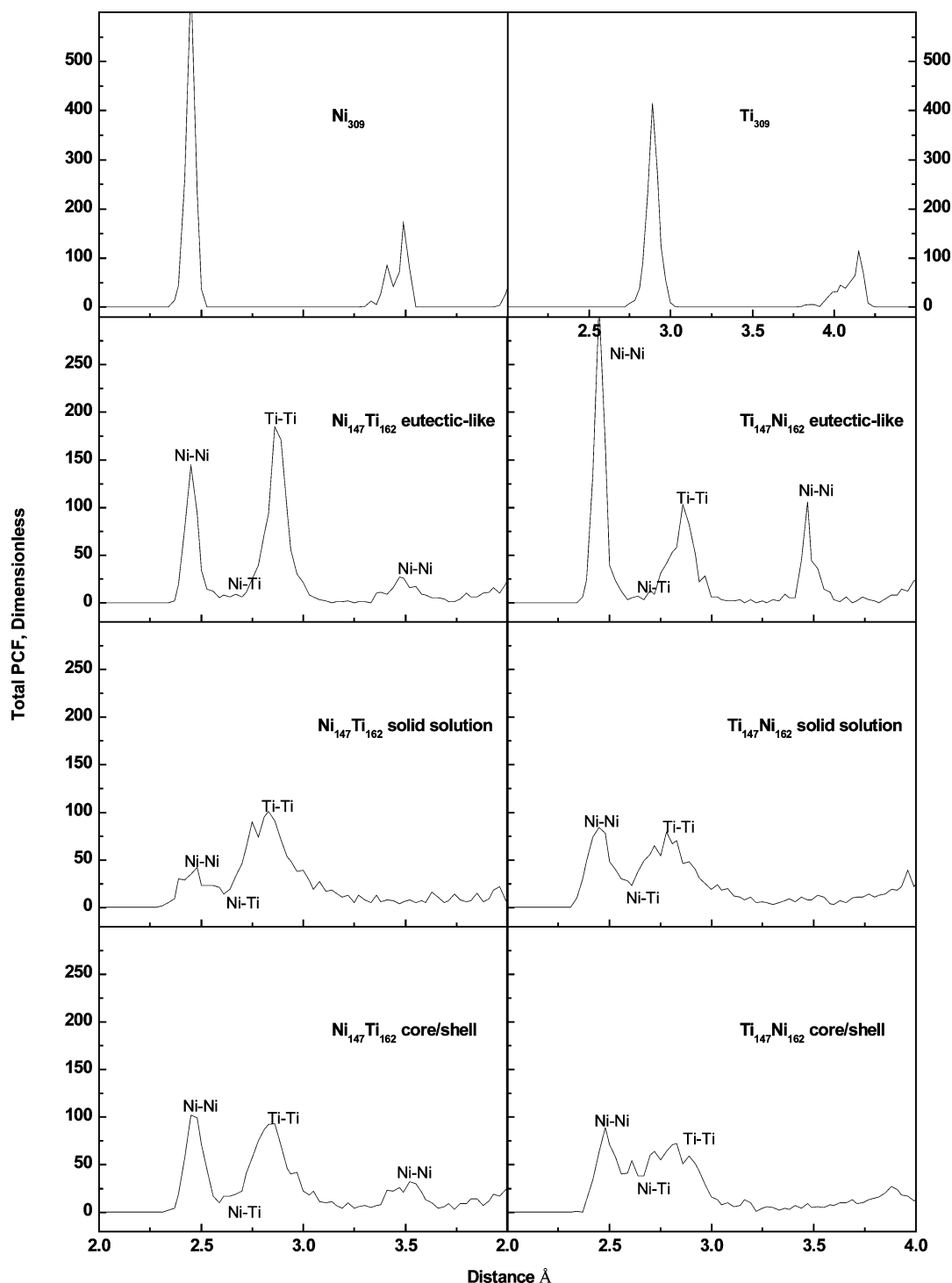
Figure 2. Total pair correlation function for 262-atom decahedron at 298 K.

tion. Actually, for some clusters with specified elemental distributions, their geometrical shape and configuration cannot persist and amorphous transition occurs. By observation of the relaxed configurations, the solid solution and Ti-core/Ni-shell structures are found to be more disordered. Of course, the order of the others decreases too, and their general structural features are retained. In the next section, further structural analysis will be carried out by pair correlation functions.

3.2. Structural Analysis. Considering amorphous transition and disordering during the relaxation of the initial model nanoclusters, pair correlation functions (PCFs) were employed to characterize the structural feature. Figures 1, 2, and 3 display the calculated total PCFs for cuboctahedra, decahedra, and

icosahedra. Besides the total PCFs, the partial PCFs for Ni–Ni, Ni–Ti, and Ti–Ti are also calculated, aiding in the analysis of elemental distribution details. In Figure 1, two typical partial PCFs are presented as inset plots for Ti-core/Ni-shell and Ti–Ni solid solutions, respectively. From Figure 1, it can be seen that the nearest neighbor and second neighbor peaks for clusters of pure Ni and pure Ti are typical for a cuboctahedron, which indicates that geometrical shape and configuration basically persist during relaxation. For eutectic-like and Ni-core/Ti-shell structures, the peaks broaden a little. By observation of the atom configurations, it is found that these clusters keep their basic structural feature; the deformation is very apparent. For solid solution and Ti-core/Ni-shell structures, the peaks broaden too
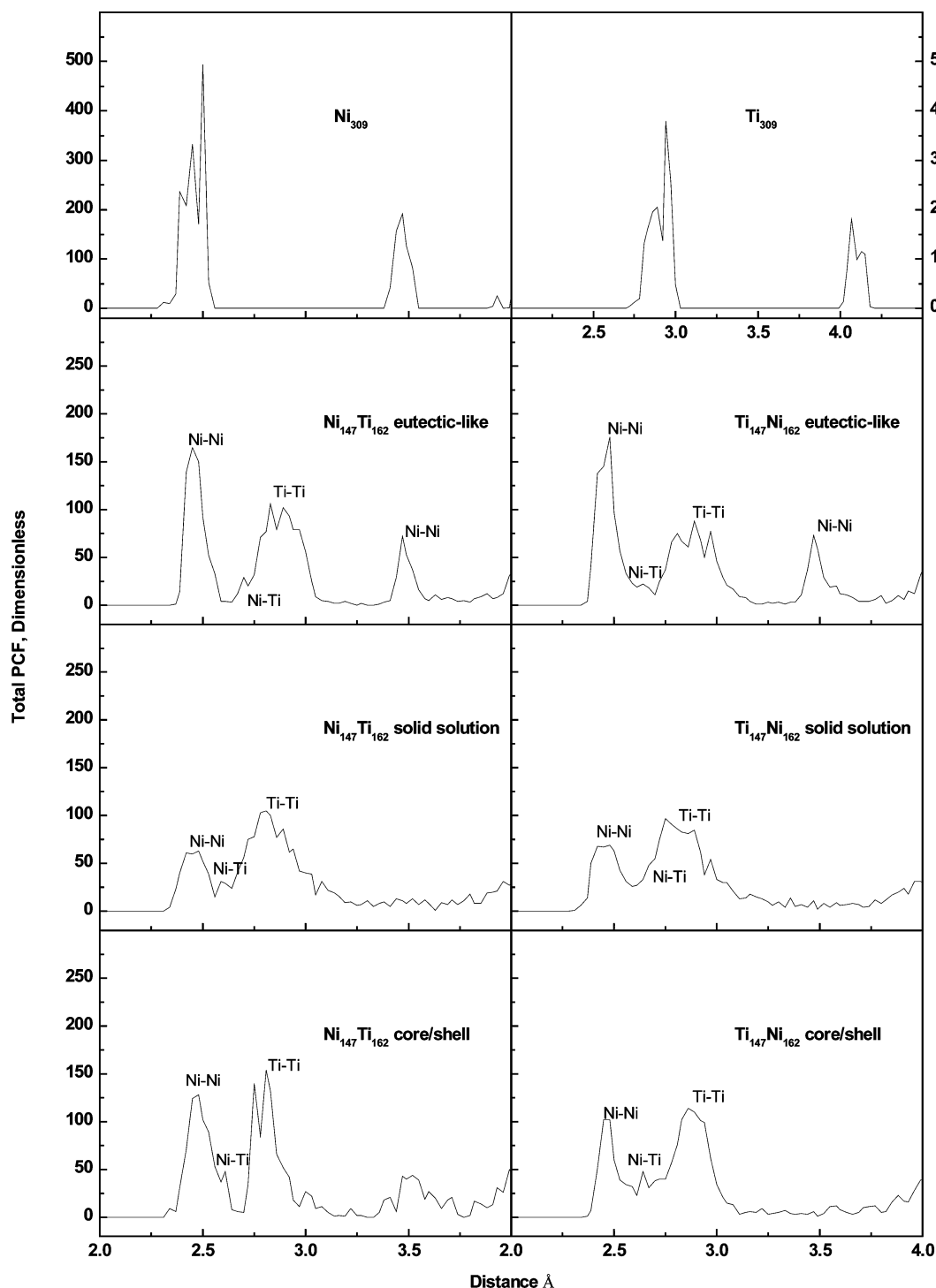
Ni−Ti Bimetallic Clusters

J. Phys. Chem. B, Vol. 110, No. 25, 2006 **12337**

Figure 3. Total pair correlation function for 309-atom icosahedron at 298 K.

much and have an amorphous feature. By analysis of the partial PCFs, the peaks of total PCFs can be distinguished roughly as the contribution of partial Ni−Ni, Ni−Ti, and Ti−Ti pairs, as marked in the plots. It must be noted that the subpeaks of Ni−Ti and Ti−Ti may overlap in a certain range of near neighboring distance, so the multipeak form of as-marked Ti−Ti subpeaks can be caused by the contribution of the subpeak of Ni−Ti. On the basis of the inset plots for Ti-core/Ni-shell and Ti−Ni solid solution, the coordination numbers can be calculated. The result demonstrates that the coordination numbers for Ni−Ni, Ni−Ti, and Ti−Ti are not of apparent difference. It means that in amorphous structures Ni and Ti tend to distribute uniformly. From another point of view, amorphous structures obtained from

different initial configurations are not identical because the atoms cannot move to wherever as they are in liquid at high temperature.

For decahedra, the solid solution and Ti-core/Ni-shell have similar behaviors with those of cuboctahedra. The peaks of Ni-core/Ti-shell become much wider; however, the subpeak of Ni−Ti is still very low. It indicates that the basic core/shell structure persists and a large deformation is generated.

For icosahedra, except for eutectic-like structures, the amorphizations occur for all the other cases. The subpeaks of Ni−Ti become apparent for core/shell structures.

Evidence of the predicted behavior are searched in produced nanoparticles by biosynthesis, which has previously been
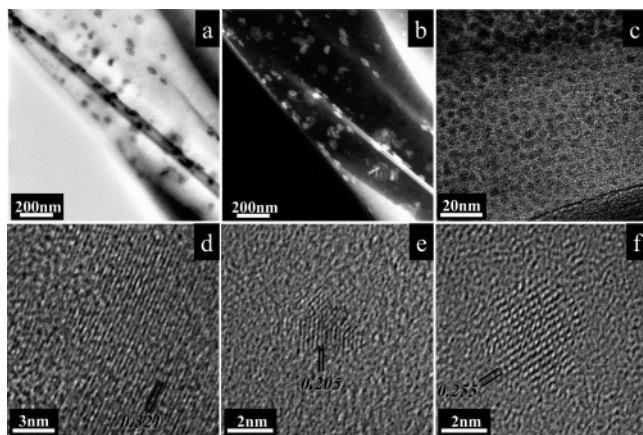
Figure 4. TEM analysis of samples with NiTi nanostructures: low magnification (a) bright field and (b) HAADF images, (c) a zone with high concentration of particles; HRTEM images of (d) a big NiTi aggregate, (e) a multiple twin Ni particle of 2.5 nm, and (f) a cubic-like Ti particle of 3.6 nm.

Figure 5. HRTEM images of NiTi nanoparticles. (a) Highly deformed cubic-like structure, (b) rounded particle with internal amorphous region, (c) axial growth deformed structure, and (d) distorted twined particle. In all the cases, the corresponding FFT is included.

reported as a successful method to generate these particles in small size. With the help of TEM techniques, the presence and structure of the clusters are studied. In Figure 4 low-resolution TEM images are used to identify the way that these particles are formed by the biomass interaction. With a bright field image (Figure 4a) we can identify the aggregates distributed along the fiber that are found in the sample. With a HAADF image (Figure 4b) we can recognize that the aggregates correspond to heavier elements than the component of the matrix. Particularly because of the high intensity of the clusters, we can determine a composition based on heavy elements. Energy dispersive spectrometry spectra were used to corroborate that the metallic composition corresponds to Ti and Ni. A higher magnification was used over a region with a high concentration of small particles, Figure 4c shows how these are partially ordered and with homogeneous particle size around 4 nm.

Higher magnification images allowed a study of the structure of particles identified in the sample, identifying a big aggregate of around 15 nm (Figure 4d), which has a interplanar spacing of 0.321 nm that corresponds to the reported cubic crystal of NiTi. Figure 4e shows a multiple twined small metallic aggregate (of diameter 2.5 nm) with measured distances of 0.205 nm that are associated to pure Ni particles. Also to a truncated octahedral cluster of 3.6 nm diameter and distances of 0.255 nm that identify it with pure Ti nanoparticles. In this way, we can establish that structures with well crystallized clusters correspond to bimetallic NiTi particles and monometallic small aggregates.

Smaller nanoparticles are found in the samples and studied by high-resolution TEM images. In Figure 5 four different particles are shown with their corresponding FFT pattern. The contrasts of these particles were commonly identified over the sample, and we selected these particular ones because of the representative evidence and that they have distances that match to the NiTi lattice spacing. In Figure 5a, a particle with square contrast can be seen but with a high deformation and the appearance of eutectic-like configurations; the FFT pattern shows weak evidence of two main reflections as expected for a square structure (see the marks). In Figure 5b a rounded particle is observed, with an internal amorphized region; the FFT shows just two dots related to parallel fringes in the cluster. An example of elongated shapes is shown in Figure 5c, which looks like a partial nanorod formation with an aspect ratio of 3, with strong distortions (marked by the arrows). In Figure 5d
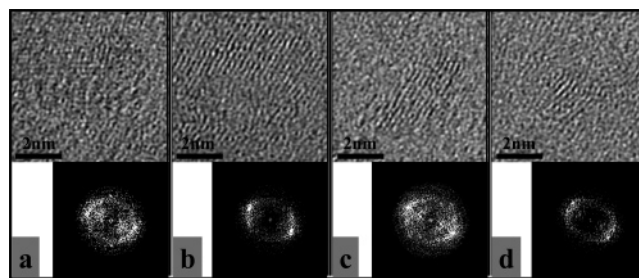
we can identify a multiple twin-like particle of 2.1 nm in a lateral view (see for instance Ascencio et al.[13]), denoting an amorphization process even in decahedral-like configurations.

Experimental evidence denotes the most stable configurations for structures with eutectic-like and partial amorphous arrays, which involves a low stability of the bimetallic crystalline aggregates. Even when the particles can be associated to both cubic and multiple twined-like configurations, the most important evidence is the minimal stability that these can have and the tendency to show a structural transition to more amorphous atomistic arrays.

4. Conclusions

By the study of molecular dynamics simulations and experimental observation on the nanoclusters synthesized by the bioreduction method, some conclusions can be drawn. In general, Ni−Ti nanoclusters as small as 2−3 nm are not energetically favorable for the common ordered geometrical arrangements as such cuboctahedron, decahedron, and icosahedron, though they can be synthesized experimentally. For the elemental distribution, the Ni and Ti tend to aggregate separately. In the cases under study, eutectic-like and Ni-core/Ti-shell structures can keep their basic shape and elemental distribution during a long period of relaxation at room temperature. For the other cases as such solid solution, Ti-core/Ni-shell, the structures amorphized and the elements tend to distribute uniformly even though they are at a temperature as low as room temperature.

References and Notes

(1) Zu, X. T.; Wan, F. R.; Zhu, S.; Wang, L. M. *Physica* **2004**, *B351*, 59.

(2) Jardine, A. P.; Field, Y.; Herman, H. *J. Mater. Sci. Lett.* **1991**, *10*, 943.

(3) Cui, L. S.; Yang, D. Z. *Trans. Met. Heat Treat.* **1994**, *15*, 39 (SYN).

(4) Liang, G. X.; Wang, E. D.; Wang, X. L. *Mater. Sci. Technol.* **1994**, *2*, 64.

(5) Liang, G. X.; Wang, E. D. *Chin. J. Mater. Res.* **1994**, *8*, 297.

(6) Porter, G. A.; Liaw, P. K.; Tiegs, T. N.; Wu, K. H. *Scr. Mater.* **2000**, *43*, 1111.

(7) Gu, Y. W.; Goh, C. W.; Goi, L. S.; Lim, C. S.; Jarforcs, A. E. W.; Tay, B. Y.; Yong, M. S. *Mater. Sci. Eng.* **2005**, *A392*, 222.

(8) Zhao, J. L.; Cui, L. S.; Gao, W. F.; Zheng, Y. J. *Intermetallics* **2005**, *13*, 301.

(9) Schabes-Retchkiman, P. S.; Canizal, G.; Herrera-Becerra, R.; Zorrilla, C.; Liu, H. B.; Ascencio, J. A. *Opt. Mater.* In press.

(10) Lai, W. S.; Liu, B. X. *J. Phys. (Paris)* **2000**, *C12*, L53.

(11) Russell, K. C. *Prog. Mater. Sci.* **1995**, *28*, 229.

(12) Massobrio, C.; Pontikis, V.; Martin, G. *Phys. Rev. B* **1990**, *41*, 10486.

(13) Liu, H. B.; Pal, U.; Medina, A.; Maldonado, C.; Ascencio, J. A. *Phys. Rev. B* **2005**, *71*, 075403.

(14) Ascencio, J. A.; Mejia, Y.; Liu, H. B.; Angeles, C.; Canizal, G. *Langmuir* **2003**, *19*, 5882.

Ni−Ti Bimetallic Clusters

J. Phys. Chem. B, Vol. 110, No. 25, 2006 **12339**

(15) Liu, H. B.; Jose-Yacaman, M.; Perez, R.; Ascencio, J. A. *Appl. Phys. A* **2003**, *76*, 63.

(16) Liu, H. B.; Pal, U.; Perez, R.; Ascencio, J. A. *J. Phys. Chem. B* **2006**, *110*, 5191.

(17) Devanathan, R.; Lam, N. Q.; Okamoto, P. R.; Meshii, M. *Phys. Rev. B* **1993**, *48*, 42.

(18) De Tendler, R. H.; Rodriguez, C.; Gallego, L. J.; Alonso, J. A. *J. Mater. Sci.* **1996**, *31*, 6395.

(19) Moine, P.; Jaouen, C. *J. Alloys Compd.* **1993**, *194*, 373.

(20) Egami, T. *J. Non-Cryst. Solids* **1996**, *205−207*, 575.

(21) Farkas, D.; Roqueta, D.; Villette, A.; Ternes, K. *Model. Simul. Mater. Sci. Eng.* **1996**, *4,* 359.

(22) Lai, W. S.; Liu, B. X. *Phys. Rev. B* **1998**, *58*, 6063

(23) Cleri, F.; Rosato, V. *Phys. Rev. B* **1993**, *48*, 22.

(24) Pasturel, A.; Colinet, C.; Nguyen, M. D.; Paxton, A. T.; van Schilfgaarde, M. *Phys. Rev. B* **1995**, *52*, 176.

(25) Hultgren, R.; Desai, P. D.; Hawkins, D. T.; Gleiser, M.; Kelly, K. K. *Selected Values of Thermodynamic Properties of Binary Alloys*; ASM: Metals Park, OH, 1973.

(26) Yu, O. E.; Valishev, M. G.; Ermakov, A. F.; Gel'd, O. V.; Petrushevsku, M. S. *Russ. J. Phys. Chem.* **1981**, *55*, 421.

(27) Riffkin, J. Simulation Center, University of Connecticut, Storrs, CT, 2006. http://ims.uconn.edu/centers/simul.